Thresholds of Plasma Formation in Silicon Identified by Optimizing the Ablation Laser Pulse Form

Hatem Dachraoui and Wolfgang Husinsky*

Institut für Allgemeine Physik, Vienna University of Technology, A-1040 Wien, Austria

(Received 18 May 2006; published 6 September 2006)

Using an evolutionary algorithm combined with pulse shaping, we have identified that rapid plasma formation in Silicon can occur already at a fluence of about 150 mJ/cm^2 if a substantial part of the laser energy is deposited efficiently around 200 fs after an exciting laser pulse. Nonthermal solid-to-liquid phase transition leads to the increase of the deposited energy in the material. Highly charged ions have been observed in the mass spectrum. While the pulse optimization procedure allowed us to identify the plasma formation, further experiments where the influence of the laser pulse width on the ablation yield was studied and Two-Pulse-Correlation experiments provided additional proof for the appearance of rapid plasma formation.

DOI: 10.1103/PhysRevLett.97.107601 PACS numbers: 79.20.Ds, 07.05.Kf, 42.62.Fi, 79.60.Bm

Despite intensive investigations and considerable progress achieved over the last years, the mechanisms of ultrashort laser ablation are still an issue of much debate. This is particularly true with respect to fast electronic processes and charging effects and how the energy is transferred to the target. The mechanisms responsible for material ejection are strongly dependent on the physical properties. of the solid, the laser fluence and, in particular, the pulse duration. In semiconductors, for example, homogeneous nucleation is estimated as the principal ablation mechanism at laser fluence just above the ablation, and plasma formation occurs only at fluences above 1 $J/cm^2 (F > 5F_{abl})$ [1]. However, the dependence of the threshold for plasma formation on the particular pulse form has not been clearly studied yet. Femtosecond (fs) Fourier-domain pulse manipulation provides a new opportunity to investigate that ablation process with respect to its dependence on the pulse form and hence its specific time dependence of the energy transfer. In this Letter, the influence of the time dependent energy transfer to a Si target is studied by maximizing (optimizing) the Si^+ ablation yield in a feedback experiment using an evolutionary algorithm [2,3], where the optimal pulse form is determined. We show that rapid plasma formation can appear at laser fluences around 150 mJ/cm^2, which is considered considerably below the reported threshold of plasma formation [1,4], if the energy is deposited over several hundred fs in a specific pulse form.

Silicon targets were irradiated in an UHV chamber (10^{-9} mbar) equipped with a reflectron-type time-of-flight (TOF) mass spectrometer. Ablation and post-ionization is performed with ultrashort laser radiation with a system consisting of two multipass colliding pulse amplifiers (CPA) Ti:sapphire amplifiers seeded from a common mode-locked Ti:sapphire oscillator. The system, operating at a repetition rate of 1 kHz, provides laser pulses at a center wavelength around 800 nm with a typical duration of 25 fs. The laser fluence could be varied between 50 mJ/cm^2 and several J/cm^2. In addition, one of the two amplifiers was equipped with an acousto-optic programmable dispersive filter (AOPDF), which allowed pulse shaping of the corresponding laser beam. Thus the pulse width of the ablating beam could be varied from 25–600 fs. The energy of the pulse was kept constant when changing the pulse width. The ablation beam was incident on the surface at an angle of 45° measured from the surface normal and was focused to a spot size of typically 100 μm in diameter. The TOF axis was normal to the target surface. The length of the TOF was about $2m$.

The evolutionary algorithm starts with an arbitrary set (generation) of pulse forms (*in the particular case, the spectral phase function determines the pulse shape*), and the following generations are selected according to an enhanced Si^+ ablation yield, which is obtained from the mass spectrum of ablated particles. Convergence is reached when the feedback signal is maximized and the optimized pulse form is found. A characteristic result of an optimization run is shown in Fig. 1(a) (150 mJ/cm^2). The result clearly shows an increase of the ion signal with generations. Arbitrary pulse forms at the beginning of the run result in low Si^+ ablation yields (Y). In Fig. 1(a) the average yield (merit function) over each generation (30 individuals) is shown. After 10 iterations, the ratio of the optimized yield Y_{op} to the initial yield Y_{in} increases typically to 2.4, which correlates with a pulse form shown in Fig. 1(b). A second important feature can also be learned from Fig. 1(c): The optimized pulse (full line, black) leads to the emission of Si^{2+} as observed in the mass spectrum. These observations are a clear indication of the beginning of a new type of ablation mechanism.

What is the nature of this mechanism? More information can be obtained by analyzing the optimized pulse and the influence of the pulse shape in general on the density of the excited electrons N_e in the conduction band at the surface, as we would expect it from existing theories. Note that at extremely high free carrier concentrations, the ablation can

 © 2006 The American Physical Society

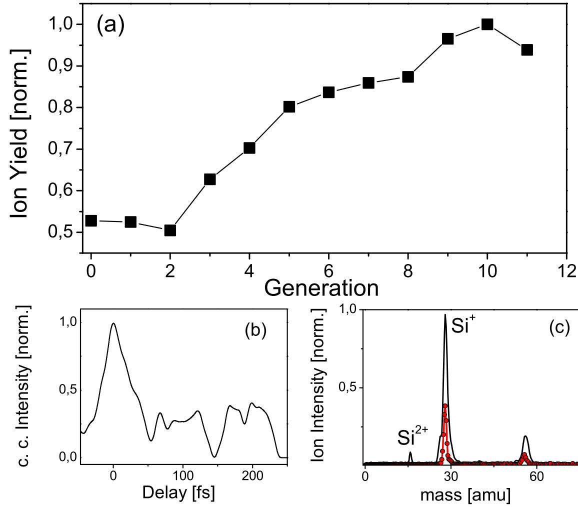

FIG. 1 (color online). (a) Evolution of the ion signal Si^+ (merit function) during optimization. (b) Cross correlation intensity of the optimal pulse. (c) The mass spectrum of the transform-limited pulse (line with circles) and the optimized pulse (solid line).

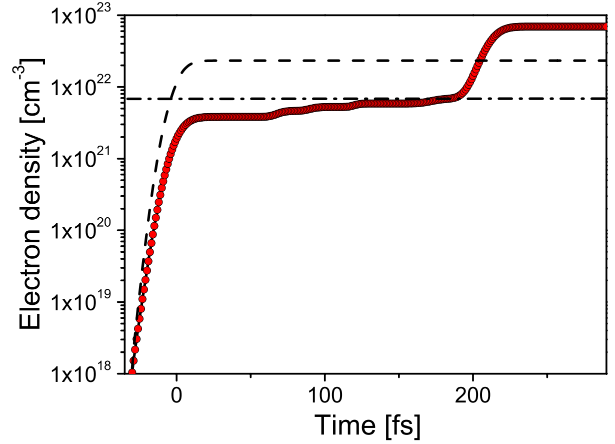

FIG. 2 (color online). Calculated electron densities (numerical solution to Eq. (1)) generated by laser excitation as functions of time for a fluence $F = 150\ \mathrm{mJ/cm^2}$: transform-limited pulse (dashed line); optimized pulse (pulse train) (solid line).

be a consequence of thermal and nonthermal ''ultrafast'' emission [5]. The optimized pulse [Fig. 1(b)] obtained by the learning algorithm roughly consists of a stronger leading pulse followed by 5 smaller pulses within 210 fs and with equal time spacing between the pulses. The energy ratio of theses pulses is about 3:1:1:1:1:1. The time evolution of the generated density of electrons N_e after femtosecond laser excitation, can be described by a rate equation [6], where the optimized pulse is approximated with a sum of time-shifted Gaussian pulses. The total energy of these pulses is compared to a single pulse with identical energy peaking at time zero. The following differential equation describes the time evolution of the electron density

$$\frac{\partial N_e}{\partial t} = \sum_i \left[\alpha + \frac{1}{2}\beta I_i(t) \right] \frac{I_i(t)}{\hbar\omega} \tag{1}$$

nonthermal where α and β describe linear and two-photon interband absorption. The spatial dependence of the laser intensity and the losses due to electron diffusion and recombination are neglected in this equation. Solving Eq. (1) with $\alpha = 3.42 \times 10^3\ \mathrm{cm}^{-1}$ and $\beta = 50 \pm 10\ \mathrm{cm/GW}$ [6], one finds that he generated electron density after the fourth subpulse rises to approximately $7 \times 10^{21}\ \mathrm{cm}^{-3}$. This is quite close to the threshold density of nonthermal melting of $10^{22}\ \mathrm{cm}^{-3}$. Because of the change of the optical properties of the semiconductor, carrier generation after the fourth pulse cannot be described with the same values of α and β. It is expected that the linear absorption coefficient increases to $\alpha_{\mathrm{liquid}} = 10^6\ \mathrm{cm}^{-1}$ and that the two-photon absorption coefficient decreases due to band gap shrinkage [7,8]. This has been taken care in the solution of Eq. (1) and the results are shown in Fig. 2. In the Figure, the development of the free-electron densities N_e after irradiation with an unshaped (single) and the optimized pulse (pulse train) are compared. The same experimental laser fluence is employed in these calculations. It becomes evident that the density of excited electrons is much larger for the optimized pulse than for the transform-limited pulse. At fluences of $150\ \mathrm{mJ/cm^2}$, the optimized pulse results in a critical electron density of $7 \times 10^{22}\ \mathrm{cm}^{-3}$. The temperature of the large derived fraction (70%) of the valence electrons to the conduction band is high enough to produce solid-plasma transition, followed by a strong surface ablation [9]. Here it should be noted that the estimated carrier temperature for this density should exceed 15,000 K [10].

Thus, the occurrence of ultrafast melting increases the absorption of the last pulse, which may lead to the starting of a further process and a stronger ablation. The observation of Si^{2+} in the mass spectrum is an indication that rapid plasma formation starts to take place when laser energy is deposited after 200 fs where the electron density exceeds the threshold for rapid plasma formation. On the other hand, we have not observed a significant change of the emission of neutral particles (*only a slight decrease*) depending on the pulse form. The decrease of the abundance of neutral particles provides additional support for our assumption.

The ratio of the flux of the emitted monomers for the optimized pulse J_{opt} and the initial transform-limited pulse J_{in} can roughly be estimated from the data in Fig. 1(c) to: $J_{\mathrm{opt}}/J_{\mathrm{in}} = 3$ [11]. According to the small signal obtained with the transform-limited pulse, we can assume that the surface temperature in this ablation regime is quite close to the threshold surface temperature for ablation of ~4000 K. Thus, a crude estimate of the surface temperature $(T_s)_{\mathrm{opt}}$ can be made using the following expressions:

$$J_{\mathrm{in}}(T_s) = \frac{b}{\sqrt{2m\pi k_B T_s}} \exp\left[-\frac{E_{A1}}{k_B T_s} \right] \tag{2}$$

$$J_{\rm opt}(T_s) = \frac{b}{\sqrt{2m\pi k_B T_s}} \exp\left[-\frac{E_{A2}}{k_B T_s}\right] \qquad (3)$$

in which E_{A1} and E_{A2} are the activation energies in the fluence domain around the ablation threshold and the plasma formation. From $E_{A1} = 1.65$ eV [1] and $E_{A2} = 4.5$ eV, we obtain $(T_s)_{\rm opt} \approx 18,000$ K.

An easier, and in many practical applications more feasible way of changing the pulse form can be realized by changing simply the pulse width of the laser pulse. In this case, the energy cannot be deposited at specific times, but can only be spread out over different time intervals. Nonetheless, studying the pulse width dependence of the Si^+ signal should yield additional information and support for the mechanisms described above. In Fig. 2 results are summarized for different laser intensities. The pulse length dependence on the yields can give indirect information on the time of the development of these processes. At the same fluence as used for the genetic pulse optimization [Fig. 1(a)], we observe almost no dependence of the Si^+ signal on the pulse width. Increasing the laser fluence, the situation significantly changes: for laser fluences of 350 and 400 mJ/cm^2, the ion yields show a significant increase at 350 and 250 fs followed by a slight decrease for pulses longer than 500 fs. On the other hand, similar to the pulse shaping measurements and described above, even at laser fluences around 400 mJ/cm^2, we have not observed a significant variation of the neutral signal with the pulse width.

For 150 mJ/cm^2, a long pulse with duration between 250–450 fs creates an electron density of (1.5–2.5) $\times 10^{21}$ cm^{-3}. This is well below the threshold density for ultrafast melting [6]. For excitations with 350 and 400 mJ/cm^2, the value of the generated free-electron density at 250 fs and 350 fs (1 and 1.5×10^{22} cm^{-3}) are equal to the density of ultrafast melting. Thus the occurrence of nonthermal melting before the end of the laser pulse is expected to lead to an increase in the absorbed energy. This explains the observed increase of the ion signal for pulse widths >250 fs (400 mJ/cm^2) and >350 fs (350 mJ/cm^2). Here it should be considered that the nonthermal, solid-to-liquid phase transition take place within few hundred femtoseconds after the excitation [12]. The faster increase of the signal at higher intensities can be explained by the increase of the duration of the solid-to-liquid phase transition with the reduction of the laser fluence. Our observations are consistent with previous x-ray measurements on Si, where it was shown, that ultrafast melting occurs later at low fluences [13].

The increase of the abundance of Si_3^+ for pulse length $\tau \geq 320$ fs (400 mJ/cm^2) supports (a) the assumption that more energy is absorbed in this stage of irradiation and (b) the starting of a new process. Typical for this process is also the characteristic emission of highly charged species (Si^{2+}, Si^{4+}) as can be seen in Fig. 3(c). In this time regime, the ablation is, therefore, caused by rapid plasma formation. Here it is important to note that various molecular

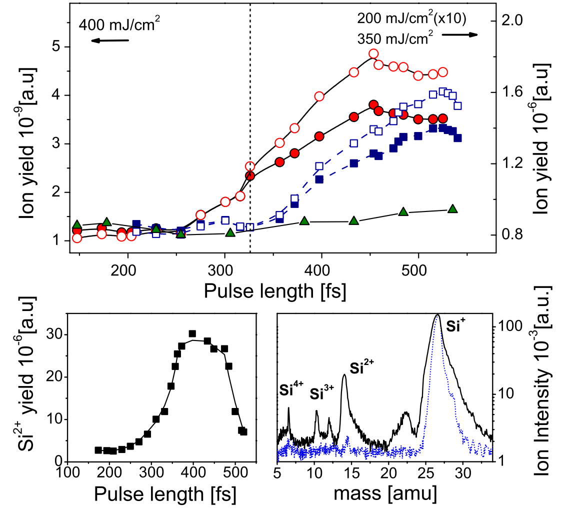

FIG. 3 (color online). (a) Pulse width dependence of the ion signal for three different laser fluences: 150 mJ/cm^2 ($Si^+ \times 10$; filled triangles), 350 mJ/cm^2 (Si^+: filled squares; $Si_3^+ \times 11$: open squares); 400 mJ/cm^2 (Si^+: filled circles; $Si_3^+ \times 11$: open circles). The dashed line at 320 fs marks the beginning of no correlation between the emission of Si^+ and Si_3^+ (for 400 mJ/cm^2). (b) Si^{2+}-yield as function of the pulse width. (c) Mass spectra for two different pulse durations: 300 fs (dotted line) and 400 fs (solid line).

desorption processes have different activation energies [14].

Plasma formation has two effects: (i) the enhancement of the absorption coefficient, which may lead to stronger ablation; (ii) dense plasma can strongly reflect laser light. This effect results in reduced ablation. This might explain the reduction of the ablation yield for pulses >500 fs due to an increased reflectivity for long pulses.

Two-Pulse-Correlation experiments allow a very specific energy deposition as a function of time. In following, we present such a pump-pump ablation experiment. Figure 4 shows the results for double-pulse ablation, where the first and second pulses have equal energies. At laser fluence exceeding the ablation threshold (120 mJ/cm^2 pro pulse), the Si^+ yield peaks for pulse delays of 300 fs. Again, this can be explained by the build up of a rapid plasma in nonthermally melted silicon. Thus, the strong coupling of the second pulse with the ultrafast molten formed by the first pulse is the origin of the occurrence of this rapid plasma. For the low laser fluence, where the laser fluence of each pulse (80 mJ/cm^2) is below the ablation threshold, there is no noticeable ablation increase because the free-electron density generated by the first pulse is still well below the critical density of ultrafast melting. On the other hand, according to [15], the observed decrease within the first 200 fs can be attributed to Coulomb-explosion.

The duration of the plasma can be estimated to 300 fs according to the gauss fit shown by the solid line. The start of the peak (250 fs) can be correlated with the time where

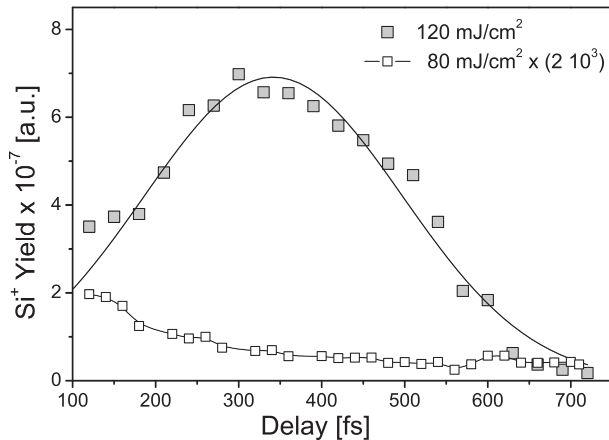

FIG. 4. Time-resolved measurements of Si^+ ion signal at two different laser fluences: 80 mJ/cm^2 (open squares) and 120 mJ/cm^2 (full squares). The solid line represent a gauss fit of the obtained experimental results at equal pump and probe pulse fluences of 120 mJ/cm^2.

the solid-to-liquid phase transition is accomplished. It is difficult to imagine that the reflection effect of the second pulse by the formed plasma is the only process responsible for the observed decrease after a delay of about 400 fs. Another possibility includes the diffusion of the generated carrier by the first pulse into the bulk. This diffusion reduces the coupling of the second pulse into the target, resulting in less ablation.

In summary, these experiments revealed the occurrence of ultrafast melting can lead to a rapid plasma formation for laser fluence around 150 mJ/cm^2, which is below the threshold of plasma formation for an arbitrary short pulses, if the laser energy is distributed in an optimized way over time. The synchronization between the temporal spacing of the subpulses and the variation of the thermodynamics and optical properties of the material increase the energy density deposited in the target. The understanding of the fundamental energy absorption mechanism and plasma development could help to optimize the generation of ultrashort extreme ultraviolet (xuv) light pulses.

The financial support of the Austrian Science Foundation FWF (Project No. P15937) is greatly acknowledged.

*Electronic address: husinsky@iap.tuwien.ac.at

[1] A. Cavalleri, K. Sokolowski-Tinten, and J. Bialkowski *et al.*, J. Appl. Phys. **85**, 3301 (1999).
[2] R. S. Judson and H. Rabitz, Phys. Rev. Lett. **68**, 1500 (1992).
[3] A. Assion, T. Baumert, M. Bergt, T. Brixner, B. Kiefer, V. Seyfried, M. Strehle, and G. Gerber, Science **282**, 919 (1998).
[4] D. von der Linde and H. Schüler, J. Opt. Soc. Am. B **13**, 216 (1996).
[5] K. Sokolowski-Tinten, J. Bialkowski, A. Cavalleri, and D. von der Linde *et al.*, Phys. Rev. Lett. **81**, 224 (1998).
[6] K. Sokolowski-Tinten and D. von der Linde, Phys. Rev. B **61**, 2643 (2000).
[7] R. Stoian and A. Mermillod-Blondin *et al.*, Appl. Phys. Lett. **87**, 124105 (2005).
[8] D. H. Reitze, T. R. Zhang, Wm. M. Wood, and M. C. Downer, J. Opt. Soc. Am. B **7**, 84 (1990).
[9] B. Rethfeld, K. Sokolowski-Tinten, and D. Von Der Linde *et al.*, Appl. Phys. A: Mater. Sci. Process. **79**, 767 (2004).
[10] M. L. Cohen and J. R. Chelikowski, *Electronic Structure and Optical Properties of Semiconductors* (Springer, Berlin, 1989).
[11] The ratio of ablation D_{opt}/D_{in} depth can be estimated of the ratio number of the emitted particles N_{opt}/N_{in} (N is proportional to the integral of all peaks in the ToF spectrum). Using the following expression: $D = \int J(T)dt$ a ratio J_{opt}/J_{in} of approximately 3 is estimated.
[12] K. Sokolowski-Tinten and D. von der Linde *et al.*, Phys. Rev. Lett. **87**, 225701 (2001).
[13] A. Rousse, C. Rischel, and S. Fourmaux *et al.*, Nature (London) **410**, 65 (2001).
[14] G. M. Rosenblatt, in *Treatise on Solid State Chemistry, Surf (I)*, edited by N. B. Hannay (Plenum, New York, 1976), Vol. 6A.
[15] H. Dachraoui, W. Husinsky, and G. Betz, Appl. Phys. A **83**, 333 (2006).